Desalination and Water Treatment
www.deswater.com
1944-3994/1944-3986 © 2012 Desalination Publications. All rights reserved
doi: 10.1080/19443994.2012.677526

46 (2012) 234–243
August

Taylor & Francis
Taylor & Francis Group

Modeling of tartrazine adsorption onto activated carbon fiber in a continuous fixed-bed reactor

Çiğdem Sarıcı-Özdemir

Faculty of Engineering, Department of Chemical Engineering, Inonu University, 44280 Malatya, Turkey
Tel. +90 422 3410010–4757; Fax: +90 422 3410046; email: cigdem.ozdemir@inonu.edu.tr

Received 6 October 2011; Accepted 12 February 2012

ABSTRACT

A column study was carried out using activated carbon fiber for the adsorption of tartrazine from aqueous solution. The effect of flow rate and inlet tartrazine concentration on the adsorption characteristics of the activated carbon fiber at 25°C was investigated. Adams–Bohart, Thomas, and Yoon-Nelson models each were applied to the experimental data to predict the breakthrough curves, and determine the characteristics and parameters of the column's usefulness for tartrazine adsorption. This study revealed that carbon fiber is suitable for use as an effective adsorbent to remove tartrazine from solution.

Keywords: Tartrazine; Fiber; Column adsorption; Thomas model

---

1. Introduction

Wastewater from textile, paper, pharmaceutical, and certain other industries contains residual dyes, especially azo dyes. It is well known that some azo dyes and their degradation products, such as aromatic amine, are highly carcinogenic. The colored wastewater released into the ecosystem is a dramatic source of esthetic pollution, and a perturbation to aquatic life. Tartrazine, an azo dye used as a foodstuff additive [1,2] and in various human drugs, has been reported as a possible cause of asthma, urticarial, and angioedema [3,4]. It also has phototoxic potential [5–7]. The estimated amounts of tartrazine manufactured in 1996 were approximately 71.35 t in Japan and 985.76 t in the USA [8]. The acceptable daily intake by human beings is 0–7.5 mg/kg body weight [5].

Dye removal from wastewater can be brought about using many techniques [9–11]. At present, the most common treatment method for the effective removal of dyestuffs from wastewater is adsorption. Adsorption is gaining increasing attention due to its simplicity of design, ease of processing, and effective removal of toxic substances. Adsorption process has been carried out using many different adsorbents. Activated carbon is an effective means for removing the toxic matter from a liquid. Activated carbon is a microporous adsorbent that can be made from a variety of carbonaceous materials [12,13]. It is a manufacturing by-product produced during the carbonization and activation of fabrics made from several polymeric materials such as nylon, phenolic resin, cellulose, etc. [14]. The activated carbon is known as activated carbon fiber (ACF) and is manufactured in two presentations as cloth and felt.

Batch reactors are easy to use in laboratory studies, but less convenient for industrial applications. On the other hand, fixed-bed columns are widely used in various chemical industries because of their simple operation [15]. Columns are an effective process for cyclic adsorption/desorption as they make the best use of the concentration difference, known to be a driving force for adsorption, and enable a more efficient utilization of the adsorbent's capacity, resulting in a better quality of effluent [16]. A large volume of solution can be continuously treated using a defined quantity of adsorbent in the column. A few investigations into dye adsorption in fixed-bed columns have reported the influence of pH, concentration of dye, flow rate, and other factors. The performance of fixed-bed columns is described by the concept of the breakthrough curve. The time of breakthrough appearance and characteristics for determining the operation and dynamic response of an adsorption column. As seen in Fig. 2, the major part of the adsorption at anytime takes place in a relatively narrow adsorption column. As the solution continues to flow, the mass transfer zero, which is S-shaped, moves down the column. The total shaded area in the total or stoichiometric capacity of the bed was calculated as follows:

$$t_t = \int_0^\infty \left(1 - \frac{C}{C_0}\right) \cdot dt \tag{1}$$

where t_t is the time equivalent to the total capacity, and C_0 and C ($mg\,L^{-1}$) are the inlet and outlet concentrations of the contaminant solution, respectively. The usable capacity of the bed up to the breakpoint time, t_b, is the crosshatched area, calculated as:

$$t_u = \int_0^{t_b} \left(1 - \frac{C}{C_0}\right) \cdot dt \tag{2}$$

where t_u is the time equivalent to the usable capacity. The value of t_u is usually very close to that of t_b.

Using the total bed length of H_T, the length of bed used up to the breakpoint H_B is calculated as:

$$H_B = \frac{t_u}{t_t} \cdot H_T \tag{3}$$

The length of unused bed H_{UNB} is then the unused fraction of the total length:

$$H_{UNB} = \left(1 - \frac{t_u}{t_t}\right) \cdot H_T \tag{4}$$

The column adsorption of tartrazine by ACF has not been investigated in previous studies. In this paper, we attempt to remove a hazardous dye, tartrazine, by using ACF as an adsorbent. ACF was wasted by chemical activation in the absence of N_2 at 500℃.

2. Materials and methods

2.1. Materials

Tartrazine is an azo dye. Fig. 1 shows the characteristics of tartrazine.

Studies were carried out by preparing a stock solution at 100 $mg\,L^{-1}$ concentration in double-distilled water. The working solutions of the desired concentrations were obtained by successive dilutions.

2.2. Preparation of ACF

ACF is produced from textile waste that is used to form felt made from polyester, nylon, and cotton.

In the first step of activation, the starting material was mixed with $ZnCl_2$ at a ratio of 0.5:1, and the mixture was kneaded after adding distilled water. The mixture was then dried at 110℃ to prepare the impregnated sample.

In the second step of activation, the impregnated sample was placed on a quartz dish, which was then inserted in to a quartz tube (i.d. = 60 mm). The impregnated sample was heated to the activation temperature (500℃) under N_2 flow (100 $mL\,min^{-1}$) at a rate of 10℃ min^{-1} and held at the activation temperature for 1 h. After activation, the sample was cooled under N_2 flow, and 0.5 N HCl was added to the activated sample. The activated sample was then washed sequentially several times with hot distilled water to remove residual chemicals, until it did not give a chloride reaction with $AgNO_3$. The washed sample was then dried at 110℃ to prepare the activated carbon [17].

A TriStar 3000 (Micromeritics, USA) surface analyzer was used to measure the nitrogen adsorption isotherm at 77 K, over a range of relative pressures from 10^{-6} to 1. The BET surface area, total pore volume, average pore radius, and micropore area were obtained from the adsorption isotherm.

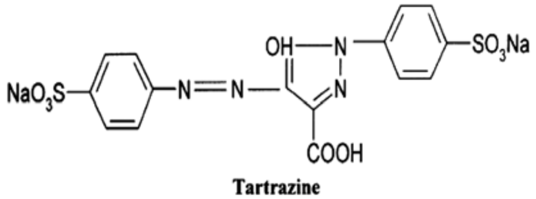

Fig. 1. Structure of tartrazine.

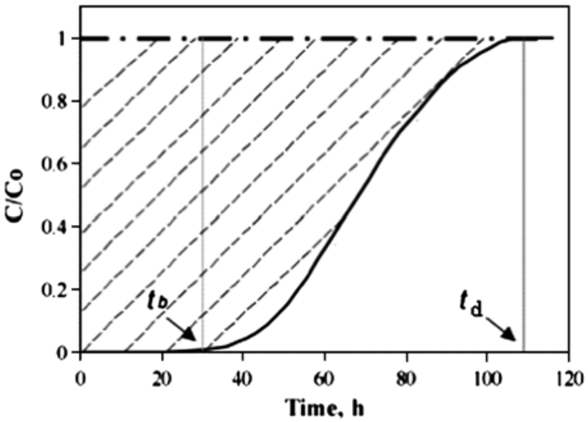

Fig. 2. Determination of column capacity from the breakthrough curve.

2.3. Column studies

Continuous fixed-bed column studies were performed using a fixed-bed mini column reactor with an inside diameter of 1.5 cm and a column height of 40 cm. The bed length used in the experiments was 6 cm. In a typical experiment, dye of a known concentration (10, 20, or 30 mg L^{-1}) was pumped at a fixed flow rate (5, 10, 20 mL min^{-1}) through the column, filled with a known bed height of adsorbent. The tartrazine solution at the outlet of the column was collected at regular time intervals, and its concentration was measured using a UV–visible spectophotometer at 426 nm [3]. All experiments were carried out at 25°C. After almost 95–98% exhaustion, the column operation was stopped.

The total quantity of tartrazine adsorbed by the column for a given inlet concentration, q_{total} (mg g^{-1}), and the flow rate, were calculated using Eq. (5) [15,16]:

$$q_{\text{total}} = \frac{Q}{1{,}000}\int_{t=0}^{t=t_{\text{total}}} C_{\text{ad}}\cdot dt \qquad (5)$$

where C_{ad} (mg L^{-1}) is the adsorbed tartrazine concentration, Q is the volumetric flow rate (mL min^{-1}), and t_{total} is the total flow time (min).

The equilibrium tartrazine uptake in the column, or the maximum capacity of the column, (q_{eq}), was defined by Eq. (6) as the total amount of tartrazine adsorbed (q_{total}) per g of the adsorbent (X) at the end of the total flow time,

$$q_{\text{eq}} = \frac{q_{\text{total}}}{X} \qquad (6)$$

Breakthrough is usually defined as the phenomenon where the effluent concentration from the column reaches about 3–5% of the influent concentration. The number of bed volumes (BV) is defined as:

$$\text{number of bed volumes} = \frac{\text{volume of solution treated}}{\text{volume of adsorbent bed}} = \frac{\text{operating time}}{\text{EBRT}} \qquad (7)$$

where the adsorbent empty bed residence time EBRT is the time required for the liquid to fill the empty column:

$$\text{EBRT} = \frac{\text{bed volume}}{\text{volumetric flow rate of the liquid}} \qquad (8)$$

The adsorbent exhaustion rate is the mass of adsorbent used per volume of liquid treated at breakthrough:

$$\text{adsorbent exhaustion rate} = \frac{\text{mass of adsorbent in column}}{\text{volume treated at breakthrough}} \qquad (9)$$

2.4. Column regeneration

The eluent selected for column regeneration was NaOH (0.1 N) due to the exceptionally good solubility of tartrazine in NaOH. Afterward, water was passed at a flow rate of 10 mL min^{-1}. It was observed that this process was sufficient for complete recovery of the dye.

3. Results and discussion

3.1. Characterization of the pore structure of the activated carbon preparation

The activated carbon prepared from waste by chemical activation with $ZnCl_2$ at 500°C for 1 h was characterized by standard methods (Table 1). The surface area, measured as a BET of 1,506 $m^2\,g^{-1}$, and the iodine number of 910 mg g^{-1}, are the highest values so far reported for activated carbons from textile waste [18,19].

The adsorption isotherm is a source of information about the porous structure of the adsorbent, the heat of adsorption, and characteristics of its physics and chemistry, among other parameters. Fig. 3 shows that the nitrogen adsorption isotherm of ACF exhibits a Type I isotherm according to the BDDT classification. The structure has decreasing microporosity. Due to the appearance of small diameter the mesopores can

Table 1
Surface properties of the ACF

Sample	S_{BET} ($m^2 g^{-1}$)	S_{Ext} ($m^2 g^{-1}$)	S_{Mic} ($m^2 g^{-1}$)	V_T ($cm^3 g^{-1}$)	D_p (nm)	Number of iodine ($mg g^{-1}$)
ACF	1,506	1,187	319	0.830	2.37	910

Mic: area of micropores.
Ext: external area.
T: total volume.

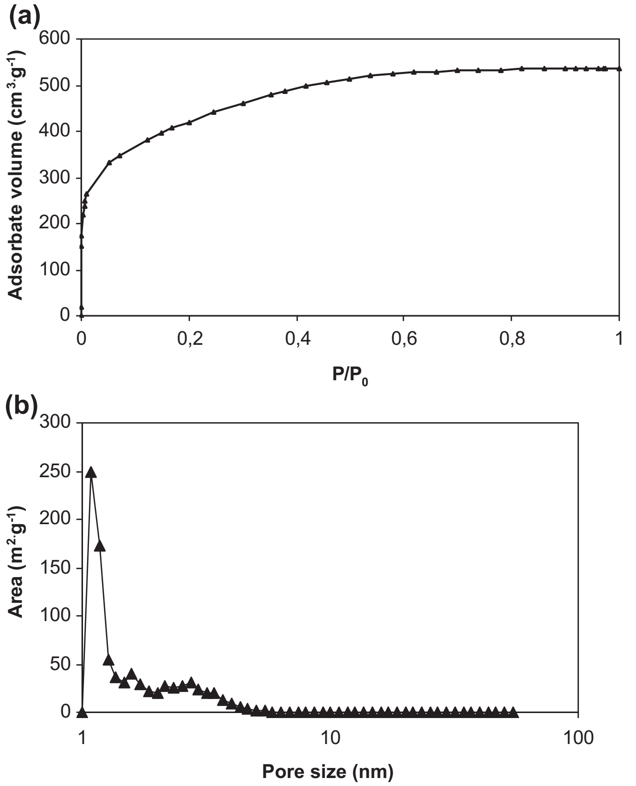

Fig. 3. Adsorption isotherm (a) and pore size distribution (b).

be physically adsorbed. The pore size distribution was calculated in the standard manner using the BJH method, as shown in Fig. 3 [20]. It appears that activated carbon, at 22%, had the highest micropore area.

3.2. Effect of the flow rate

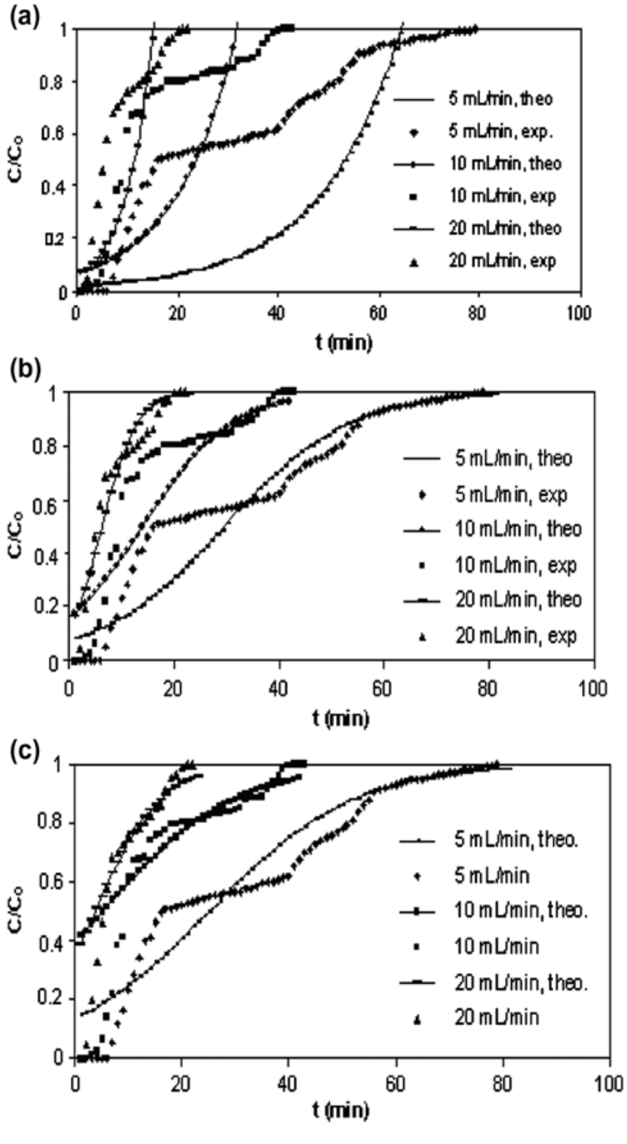

Fig. 4. Effect of flow rate on breakthrough curve and theoretical curves.

Flow rate is an important parameter for evaluating the efficiency of adsorbents for the continuous treatment processing of effluents on a pilot or industrial scale. To investigate the effect of flow rate on the adsorption of tartrazine by ACF, the inlet dye concentration in the feed was held constant at 20 $mg L^{-1}$ while the flow rate was varied from 5 to 20 $mg min^{-1}$. Fig. 4 depicts the breakthrough curves C/C_0 vs. time t. As indicated in Fig. 4, at the lowest flow rate of 5 $mL min^{-1}$, relatively higher uptake values were observed for tartrazine adsorption onto activated carbon at the beginning of the column's operation. Furthermore, as the solution continued to flow, the concentration of tartrazine in the effluent was found to increase rapidly, the bed became saturated with tartrazine, and the concentration of the solute in the effluent suddenly increased to the inlet tartrazine concentration.

As shown in Table 2, the breakthrough occurred (t_d) at 81, 39, and 19 min, and H_B investigated at 1.32, 1.11, and 1.14 cm, at flow rates of 5, 10, and 20 mL min^{-1}, respectively. The maximum bed capacities for flow rates of 5, 10, and 20 mL min^{-1} were found to be 8.1, 7.8, and 7.22 mg g^{-1}, respectively. It was observed that as the flow rate increased, the breakthrough curve became increasingly steeper. However, the breakpoint time and concentration of the adsorbed dye decreased. This behavior could be explained by positing that the effective dye concentration in activated carbon fiber is affected by inadequate residence time of the solute in the column, diffusion of the solute into pores of the activated carbon, or a limited number of active sites.

Table 2 depicts the EBRT as 2.12, 1.06, and 0.53; BV as 38.21, 36.79, and 35.84; and the adsorbent exhaustion rates as 2.4, 5.12, and 10.52 (%), for flow rates of 5, 10, or 20 mL min^{-1}, respectively. It was also observed that as the flow rate increased, the adsorbent exhaustion rate increased. Thus, at higher EBRT, tartrazine ions have more time to remain in contact with the activated carbon fiber, which results in a higher rate of removal of tartrazine molecules in the fixed-bed column. The level of tartrazine uptake was found to increase slightly with an increase in EBRT. However, removal seemed to be the same if concentration vs. bed volumes were plotted. It should be mentioned that the insignificant difference between the EBRT values is the major reason for this observation. The EBRT effect can be important for dye removal if the values are changed dramatically. BV is a function of the properties of the solutions and the carbons. With the lower EBRT, the dye molecules do not have sufficient time to react with the functional groups. At the same time, dispersion and advection in the dye transfer become important at lower EBRT. On the other hand, BV can increase when the EBRT increases [21,22].

3.3. *Effect of inlet dye concentration*

Adsorption experiments were conducted in fixed-bed columns with varying concentrations of the influent dye. Fig. 5 depicts the effect of variations in the inlet concentration of the solution used ranging from 10 to 30 mg L^{-1}, at a linear flow rate of 10 mL min^{-1}. It can be seen that a rise in the inlet dye concentration reduces the volume treated prior to saturation of the

Table 2
Column data and parameters obtained at different flow rates and concentrations

Flow rate (mL min^{-1})	Concentration (mg L^{-1})	t_d (min)	t_t (min)	t_b (min)	H_B (cm)	H_{UNB} (cm)	q_e (mg g^{-1})	EBRT	BV	Exh. rate (%)
5	20	81	45.5	10	1.32	4.68	4.05	2.12	38.21	2.40
10	20	39	21.5	4	1.11	4.89	3.90	1.06	36.79	5.12
20	20	19	10.5	2	1.14	4.86	3.61	0.53	35.84	10.52
10	10	43	25	7	1.68	4.32	2.15	1.06	40.57	4.65
10	30	34	18	2	0.67	5.33	5.10	1.06	32.05	5.88

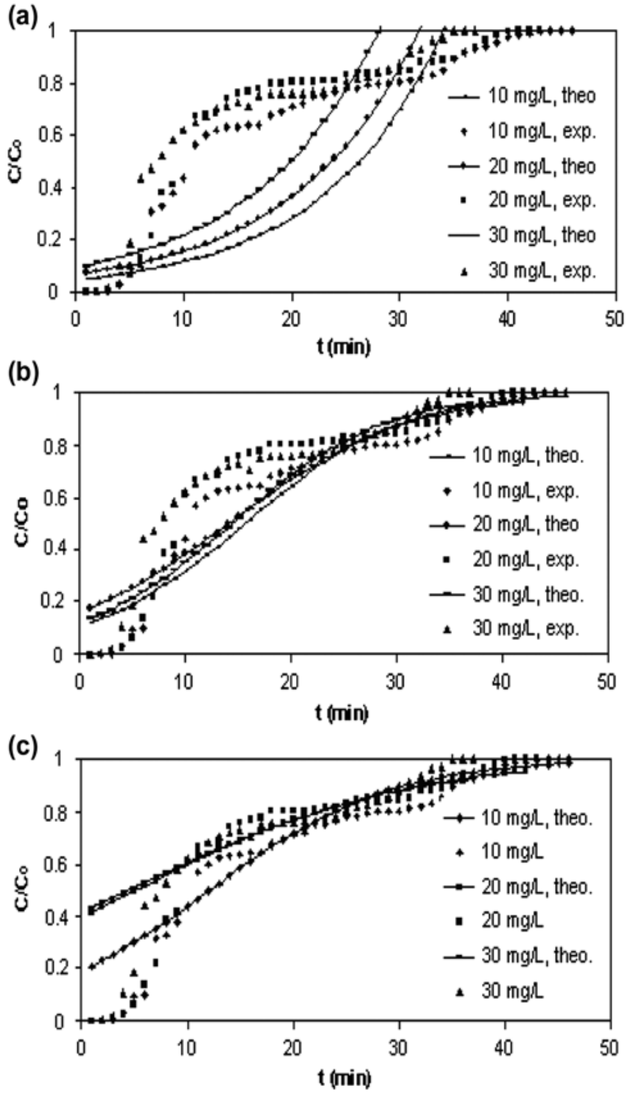

Fig. 5. Effect of initial tartrazine concentration on breakthrough curve and theoretical curves.

packed bed, as shown in Table 2. A high dye concentration might saturate the activated carbon fiber more quickly, thereby decreasing the breakthrough time. Similar results were obtained for the adsorption of tartrazine onto bottom ash and de-oiled soya [4], and for adsorption onto polystyrene anion exchangers [24]. The maximum adsorption capacity of activated carbon fiber is 5.10 mg g^{-1} at an inlet tartrazine concentration of 30 mg L^{-1}. The driving force for adsorption is the concentration difference between the solute on the adsorbent and the solute in the solution. A high concentration difference produces a high driving force for the adsorption process. This could explain the various higher adsorption capacities that were achieved in the column fed with a higher dye concentration.

3.4. Modeling of the breakthrough curves

Different equations derived for model adsorption for theoretical purposes are differential in nature and usually require complex numerical methods to achieve a solution. Such a numerical solution is usually not difficult, but often does not fit with the experimental results especially well. Various simple mathematical methods have been developed to predict the dynamic behavior of the column: the following models characterizing fixed-bed performance have been examined [23–25].

The Adam–Bohart adsorption model was applied to describe the initial part of the breakthrough curve. In this model, it is assumed that the adsorption rate is proportional both to the residual capacity of the activated carbon and to the concentration of the adsorbing species. The mass transfer rates obey the following equations:

$$\frac{dq}{dt} = -k_{\mathrm{AB}} \cdot q \cdot C_{\mathrm{AB}} \tag{10}$$

$$\frac{dC_{\mathrm{b}}}{dz} = \frac{-k_{\mathrm{AB}}}{U_0} \cdot q \cdot C_{\mathrm{b}} \tag{11}$$

where k_{AB} is the kinetic constant (L mg^{-1} min^{-1}). Some assumptions are made for the solutions of these differential equation systems such as:

(i) the concentration field is considered to be low, e.g. effluent concentration $C < 0.15\ C_0$
(ii) for $t \rightarrow \infty$ $q \rightarrow N_{\mathrm{o}}$ (where N_0 is the solution concentration (mg L^{-1})).

The differential equation system for solving the following equation is obtained from parameters k_{AB} and N_0:

$$\ln\frac{C}{C_0} = k_{\mathrm{AB}} \cdot C_0 \cdot t - k_{\mathrm{AB}} \cdot N_0 \frac{z}{U_0} \tag{12}$$

where Z is the bed depth (mm), U_0 is the superficial liquid velocity based on the empty column (mm min^{-1}), and C_0 and C are the inlet and effluent tartrazine concentrations (mg L^{-1}), respectively [16,26,27].

The Thomas solution is one of the most generally and widely used methods in the column performance theory. The model has the following form:

$$\frac{C}{C_0} = \frac{1}{1 + \exp\left(\frac{k_{\mathrm{TH}}}{Q}(q_0 \cdot X - C_0 \cdot V_{\mathrm{eff}})\right)} \tag{13}$$

where k_{TH} is the Thomas rate constant (mL min^{-1} mg^{-1}) and q_0 is the maximum solid-phase concentration of the solute (mg g^{-1}). The linearized form of the Thomas model is given as follows:

$$\ln\left(\frac{C_0}{C}-1\right)=\frac{k_{TH}\cdot q_e\cdot X}{Q}-\frac{k_{TH}\cdot C_0}{Q}\cdot V_{eff} \tag{14}$$

The Thomas or reaction model, which assumes Langmuir kinetics of adsorption/desorption and no axial dispersion, is derived from the assumption that the rate-driving force obeys second-order reversible reaction kinetics [28].

Yoon and Nelson also developed a relatively simple model to address the adsorption and breakthrough of adsorbate vapors of gases with respect to activated charcoal. This model is based on the assumption that the rate of decrease in the probability of adsorption for each adsorbate molecule is proportional to the probability of adsorbate adsorption, and the probability of adsorbate breakthrough on the adsorbent. The Yoon and Nelson equation relating to a single-component system is expressed as:

$$\ln\frac{C}{C_0-C}=k_{YN}\cdot t-\tau\cdot k_{YN} \tag{15}$$

where k_{YN} is the rate constant (min^{-1}), τ is the time required for 50% adsorbate breakthrough (min), and t is the breakthrough (sampling) time (min) [25].

The Adam–Bohart, Thomas, and Yoon–Nelson models were each fitted employing the nonlinear fitting method. The most appropriate theoretical models that describe the experimental data of the dye-activated carbon system were chosen from the R^2 value. In this study, the values of ε were determined as follows:

$$\varepsilon=\frac{\sum_{i=1}^{N}\left[\frac{(C/C_0)_{exp}-(C/C_0)_{th}}{(C/C_0)_{exp}}\right]}{N}\cdot 100 \tag{16}$$

where N is the number of measurements.

3.5. Application of the Adams–Bohart model

The Adams–Bohart model is focused on the investigation of characteristic parameters such as maximum adsorption capacity (N_0) and kinetic constant (k_{AB}). The respective values of N_0 and k_{AB} were calculated from the $\ln C/C_o$ vs. t plots at each flow rate, and each inlet tartrazine concentration studied, and are presented in Table 3. It was observed that the values of the kinetic constant increased with increasing flow rate and decreasing tartrazine concentration, and the value of N_0 increased. This indicates that the adsorption kinetics are dominated by external mass transfer in the initial part of adsorption by the column. The breakthrough curves predicted from the Adams–Bohart model were compared with the experimental points, and are shown in Figs. 4 and 5, which are clear from the values and average percentage errors in Table 3. It can be seen that the values of average percentage errors increased with increasing flow rate and decreasing tartrazine concentration. Further, there was good agreement between the experimental and predicted values, suggesting that the Adams–Bohart model is valid for dye adsorption in cases where the relative concentration region reaches up to 0.5 under all operating conditions.

3.6. Application of the Thomas model

The Thomas model was fitted to investigate the breakthrough behavior of tartrazine onto ACF. The Thomas rate constant (k_{Th}) and the maximum solid-phase concentration (q_0) were obtained using nonlinear regression analysis according to Eq. (14). Application of the Thomas model to the data at C/C_0 ratios higher than 0.07, or lower than 0.98, with respect to the flow rate and inlet dye concentrations, enabled determination of the kinetic coefficient in the adsorption system. Analysis of the regression coefficients indicated that the regressed lines provided a good fit to the experimental data, with R^2 values ranging from 0.91 to 0.97. The values of k_{Th} and q_0 are presented in Table 4. It can be seen that as the flow rate increased,

Table 3
Adams–Bohart model parameters at different flow rates and inlet concentrations

Flow rate (mL min^{-1})	Concentration (mg L^{-1})	$k_{AB}\cdot 10^3$ (L mg^{-1} min^{-1})	N_0 (mg L^{-1})	β_a (min^{-1})	R^2	ε (%)
5	20	3.14	12.13	0.038	0.910	5.14
10	20	4.24	11.99	0.050	0.987	33.92
20	20	9.22	11.47	0.105	0.918	35.65
10	10	8.92	6.40	0.057	0.955	37.36
10	30	2.81	18.66	0.052	0.944	29.38

Table 4
Thomas model parameters at different flow rates and inlet concentrations

Flow rate (mL min^{-1})	Concentration (mg L^{-1})	k_{Th} (mL mg^{-1} min^{-1})	$q_{0,cal}$ (mg g^{-1})	$q_{0,exp}$ (mg g^{-1})	R^2	ε (%)
5	20	4.24	2.50	4.05	0.955	11.44
10	20	5.93	2.01	3.90	0.906	13.99
20	20	15.20	1.97	3.61	0.930	21.46
10	10	13.16	1.28	2.15	0.910	16.01
10	30	4.59	2.76	5.10	0.970	12.14

Table 5
Yoon-Nelson model parameters at different flow rates and inlet concentrations

Flow rate (mL min^{-1})	Concentration (mg L^{-1})	k_{YN} (L min^{-1})	τ_{theo} (min)	τ_{theo} (min)	R^2	ε (%)
5	20	0.073	25.41	18	0.925	14.62
10	20	0.080	5.18	9	0.922	16.24
20	20	0.163	3.77	5	0.930	17.32
10	10	0.118	12.18	10	0.935	20.92
10	30	0.076	4.52	7	0.911	15.73

the values of k_{Th} increased and the values of q_0 decreased. Furthermore, the bed capacity q_0 increased, and the coefficient k_{Th} decreased with increasing tartrazine concentration. The trend of q_{eq}(exp) change is familiar with that of q_0. Furthermore, the value of q_0 obtained from the experiment was different from the result calculated for the same conditions. It is clear from Figs. 4 and 5 that although the model gave a poor fit of the experimental data at higher flow rates, there was good agreement between the experimental and predicted normalized concentration values at all tartrazine inlet concentrations.

Thus, it can be concluded that the Thomas model is suitable for the tartrazine adsorption process in cases where external and internal diffusions will not be the limiting step.

3.7. Application of the Yoon–Nelson model

A simple theoretical model developed by Yoon–Nelson was applied to investigate the breakthrough behavior of tartrazine on activated carbon fiber. The values of k_{YN} and τ were determined at different flow rates varying between 5 and 20 mL min^{-1}, and at different inlet tartrazine concentrations varying between 10 and 30 mg L^{-1}. It can be seen from Table 5 that the rate constant k_{YN} increased with increasing flow rate and decreased with increasing inlet tartrazine concentration. Furthermore, the values of τ decreased both with increasing flow rate and tartrazine concentration. The data in Table 5 also indicate that the τ values are very similar to the experimental results. The theoretical curves are compared with the corresponding experimental data in Figs. 4 and 5. It can be seen that the experimental breakthrough curves are very close to those predicted by the Yoon–Nelson model in the C/C_0 region from 0.06 up to 0.99. Thus, it is clear from the figures and the average percentage errors (<20.92%) in Table 5 that there is good agreement between the experimental values and the predicted values obtained from the experimental results and data regression. The model proposed by Yoon-Nelson provided a good correlation of the effect of inlet tartrazine concentration and flow rate.

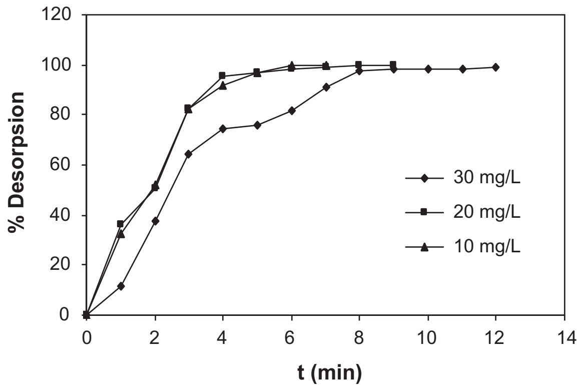

Fig. 6. Desorption curves of tartrazine at different initial concentrations.

3.8. Desorption of tartrazine and regeneration of ACF

Disposal of the exhausted adsorbent loaded with dye ions can create another environmental problem, as it is a hazardous material that pollutes the environment. Regeneration of the adsorbent material is of crucial importance for the economic development of this process.

Once the column reaches exhaustion level, it is important to be able to regenerate the ACF in order to recover the dye ions, as well as to reuse the ACF for adsorption. A fixed-bed column regeneration study was conducted to assess the possibilities for reuse of the adsorbent, and recovery of dye ions at different inlet tartrazine concentrations. The exhausted ACF was regenerated using NaOH solution. Next the column was washed with distilled water. Fig. 6 shows the desorption. It can be seen that desorption time increased with increasing dye concentration. Desorption at 8, 10, and 12 min for inlet tartrazine concentrations of 10, 20, and 30 mg L^{-1}, respectively, is shown in Fig. 6.

4. Conclusions

In this study, experimental and theoretical investigations were carried out to evaluate the performance of a fixed-bed column for removing tartrazine from aqueous solution onto ACF. The following conclusions were drawn:

- The adsorption of tartrazine is dependent on both the flow rate and inlet tartrazine concentration; the breakpoint time and tartrazine removal yield decrease with increasing flow rate and tartrazine concentration.
- The Adams–Bohart, Thomas, and Yoon–Nelson models were applied to the experimental data obtained from dynamic studies performed on a fixed column in order to predict breakthrough curves and determine the column's kinetic parameters. The model constants belonging to each model were determined by linear regression techniques and were proposed for use in column design.
- Tartrazine was easily desorbed from the ACF column using NaOH and water. The ACF column could be reused to remove tartrazine from aqueous solution efficiently.
- The results also indicated that the adsorption process could only deal with lower flow rates and lower concentrations of tartrazine solutions, if a high percentage of removal was required for extended periods. By adjusting the operating characteristics of the packed column, for example the flow rate, temperature, inlet tartrazine concentration, pH, particle size, and bed height can be achieved for the system.

Nomenclature

C_0 — inlet concentration (mg L^{-1})
C — outlet concentration (mg L^{-1})
t_t — total time (min)
t_b — breakpoint time (min)
t_u — equivalent time (min)
H_T — total bed length (cm)
H_B — breakpoint length (cm)
H_{UNB} — unused fraction of the total length (cm)
q_{total} — total amount of tartrazine adsorbed (mg g^{-1})
C_{ad} — adsorbed tartrazine concentration (mg L^{-1})
Q — volumetric flow rate (mL min^{-1})
q_{eq} — maximum capacity of the column (mg g^{-1})
X — amount of adsorbant (g)
k_{AB} — Adams–Bohart kinetic constant (L mg^{-1} min^{-1})
N_0 — solution concentration (mg L^{-1})
U_0 — superficial liquid velocity (mm min^{-1})
Z — bed depth (mm)
k_{TH} — Thomas rate constant (mL min^{-1} mg^{-1})
k_{YN} — Yoon-Nelson rate constant (min^{-1})
τ — time required for 50% adsorbate breakthrough (min)

References

[1] A. Tarrega, E. Costell, Colour and consistency of semi-solid dairy desserts: Instrumental and sensory measurements, J. Food Eng. 78 (2007) 655–661.

[2] E.V. Hess, Environmental chemicals and autoimmune disease: cause and effect, Toxicology 181 (2002) 65–70.

[3] A. Mittal, L. Kurup, J. Mittal, Freundlich and Langmuir adsorption isotherms and kinetics for the removal of tartrazine from aqueous solutions using hen feathers, J. Hazard. Mater. 146 (2007) 243–248.

[4] A. Mittal, J. Mittal, L. Kurup, Adsorption isotherms, kinetics and column operations for the removal of hazardous dye, tartrazine from aqueous solutions using waste materials bottom ash and de-oiled soya, as adsorbents, J. Hazard. Mater. 136 (2006) 567–578.

[5] T. Tanaka, Reproductive and neurobehavioral toxicity study of tartrazine administered to mice in the diet, Food Chem. Toxicol. 44 (2006) 179–187.

[6] M.S. Bhatia, Allergy to tartrazine in psychotropic drugs, J. Clin. Psychiatry 61 (2000) 473–476.

[7] L. Rosenhall, Evaluation of intolerance to analgesic, preservatives and food colorants with challenge tests, Eur. J. Respir. Dis. 63 (1982) 410–419.

[8] S. Ishimitsu., I. Mishima, S. Tsuji, T. Shibata, Comparison of estimated production of coal-tar dyes in Japan and USA, Food Sanitat. Res. 48 (1998) 33–40.

[9] A. Atia, M. Donia, A. Rashad, Efficient adsorption of malathion from different media using thermally treated kaolinite, Desalin. Water Treat. 30 (2011) 178–185.

[10] C.L. Yang, J. McGarrahan, Electrochemical coagulation for textile effluent decolorization, J. Hazard. Mater. 127 (2005) 40–47.

[11] J. Chunga, J. Kimb, Application of advanced oxidation processes to remove refractory compounds from dye wastewater, Desalin. Water Treat. 25 (2011) 233–240.

[12] Ç. Şentorun-Shalaby, M. Uçak-Astarlıoğlu, L. Artok, Ç. Sarıcı, Preparation and characterization of activated carbons by one step-steam pyrolysis/activation from apricot stones, Micropor. Mesopor. Mater. 88 (2006) 126–134.

[13] M.M.A. El-Latif, A.M. Ibrahim, Removal of reactive dye from aqueous solutions by adsorption onto activated carbons prepared from oak sawdust, Desalin. Water Treat. 20 (2010) 102–113.

[14] R. Leyva-Ramos, P. Diaz-Flores, J. Leyva-Ramos, R. Femat-Flores, Kinetic modeling of pentachlorophenol adsorption from aqueous solution on activated carbon fibers, Carbon 45 (2007) 2280–2289.

[15] J.P. Chen, M.S. Lin, Equilibrium and kinetics of metal ion adsorption onto a commercial H-type granular activated carbon; experimental and modeling studies, Water Res. 35 (2001) 2385–2394.

[16] Z. Aksu, F. Gönen, Biosorption of phenol by immobilized activated sludge in a continuous packed bed: Prediction of breakthrough curves, Process Biochem. 39 (2004) 599–613.

[17] O. Ioannidou, A. Zabaniotu, Agricultural residues as precursors for activated carbon production, Renew. Sustain. Energy Rev. 11 (2007) 1966–2005.

[18] P.T. Williams, A.R. Reed, Pre-formed activated carbon matting derived from the pyrolysis of biomass natural fibre textile waste, J. Anal. Appl. Pyrolysis 70 (2003) 563–577.

[19] M.C. Blanco López, A. Martínez-Alonso, J.M.D. Tascón, Microporous texture of activated carbon fibers prepared from Nomex aramid fibres, Micropor. Mesopor. Mater. 34 (2000) 171–179.

[20] P.E.P. Barrett, L.G. Joyner, P.P. Halenda, The determination of pore volume and area distribution in porous substance. I. Computations from nitrogen isotherms, J. Am. Chem. Soc. 73 (1951) 373–380.

[21] J.P. Chen, Effects of chemical and physical properties of influent on copper sorption onto activated carbon fixed-bed columns, Carbon 41 (2003) 1635–1644.

[22] B. Kuman, A. Kaushik, Cyanobacterial biosorption of Cr(IV): Application of two parameter and Bohart Adams models for batch and column studies, Chem. Eng. J. 144 (2008) 391–399.

[23] M. Wawrzkiewicz, Z. Hubicki, Removal of tartrazine from aqueous solutions by strongly basic polystyrene anion exchange resins, J. Hazard. Mater. 164 (2008) 502–509.

[24] J.R. Rao, T. Viraraghavan, Biosorption phenol from aqueous solution by *Aspergillus niger* biomass, Bioresour. Technol. 85 (2002) 165–171.

[25] Y.H. Yoen, J.H. Nelson, Application of gas adsorption kinetics I. A theorical model for respiratör cartridge service time, Am. Ind. Assoc. J. 45 (1984) 509–516.

[26] A.C. Texier, Y. Andres, C. Four-Brasquet, P. Le Cloirec, Fixed bed study for lanthanide (La, Eu, Yb) ions removal from aqueous solutions immobilized *Pseudomonas aeruginosa* experimental data and modelization, Process. Biochem. 47 (2002) 333–342.

[27] A. Wolborska, Adsorption on activated carbon of *p*-nitrophenol from aqueous solution, Water Res. 23 (1989) 85–91.

[28] H.C. Thomas, Heterogeneous ion exchange in a flowing system, J. Am. Chem. Soc. 66 (1944) 1664–1666.